We are IntechOpen, the world's leading publisher of Open Access books Built by scientists, for scientists

6,900
Open access books available

185,000
International authors and editors

200M
Downloads

Our authors are among the

154
Countries delivered to

TOP 1%
most cited scientists

12.2%
Contributors from top 500 universities

WEB OF SCIENCE™

Selection of our books indexed in the Book Citation Index in Web of Science™ Core Collection (BKCI)

Interested in publishing with us?
Contact book.department@intechopen.com

Numbers displayed above are based on latest data collected.
For more information visit www.intechopen.com

Chapter 6

Interference Alignment in Multi-Input Multi-Output Cognitive Radio-Based Network

Arif Basgumus, Mustafa Namdar, Hakan Alakoca, Eylem Erdogan and Lutfiye Durak-Ata

Additional information is available at the end of the chapter

http://dx.doi.org/10.5772/intechopen.80073

Abstract

This study investigates the interference alignment techniques for cognitive radio networks toward 5G to meet the demand and challenges for future wireless communications requirements. In this context, we examine the performance of the interference alignment in two parts. In the first part of this chapter, a multi-input multi-output (MIMO) cognitive radio network in the presence of multiple secondary users (SUs) is investigated. The proposed model assumes that linear interference alignment is used at the primary system to lessen the interference between primary and secondary networks. Herein, we derive the closed-form mathematical equations for the outage probability considering the interference leakage occurred in the primary system. The second part of this study analyzes the performance of interference alignment for underlay cognitive two-way relay networks with channel state information (CSI) quantization error. Here, a two-way amplify-and-forward relaying scheme is considered for independent and identically distributed Rayleigh fading channel. The closed-form average pairwise error probability expressions are derived, and the effect of CSI quantization error is analyzed based on the bit error rate performance. Finally, we evaluate the instantaneous capacity for both primary and secondary networks[*].

Keywords: 5G wireless communication systems, average pairwise error probability, CSI quantization, cognitive radio networks, interference alignment, MIMO, outage probability performance, two-way amplify-and-forward relaying

[*]The content of this study has partially been submitted in IEEE 41st International Conference on Telecommunications and Signal Processing (TSP 2018).

IntechOpen

© 2018 The Author(s). Licensee IntechOpen. This chapter is distributed under the terms of the Creative Commons Attribution License (http://creativecommons.org/licenses/by/3.0), which permits unrestricted use, distribution, and reproduction in any medium, provided the original work is properly cited. CC BY

1. Introduction

The rapidly growing number of mobile devices, higher data rates and cellular traffic, and quality of service requirements trigger the development of mobile communications. It is expected that the next-generation cellular networks (5G and beyond) will meet the advanced technology requirements. 4G networks are not powerful enough to support massively connected devices with low latency and high spectral efficiency, which is critical for next-generation networks. 5G networks are characterized by three fundamental functions in general: connectivity for everywhere, low latency for communication, and very high-speed data transmission [1].

In the near future, a large number of mobile devices will connect to one another in everywhere and provide a seamless mobile user experience. Real-time applications and critical systems and services (medical applications, traffic flow, etc.) with zero latency are expected to be offered over 5G cellular networks. Besides, the fast data transmission and reception will be ensured by supporting zero latency using a high-speed link. For this reason, the scope of 5G cellular networks bring the emerging advantages, new architectures, methodologies, and technologies on telecommunications such as energy-efficient heterogeneous networks, software-defined networks (SDN), full-duplex radio communications, device-to-device (D2D) communications, and cognitive radio (CR) networks. An increasing number of mobile devices and the bandwidth requirement for large amounts of data require the development of the new technologies and infrastructures in addition to the existing technology. It is inevitable that the number of smart phones, high-definition televisions, cameras, computers, transport systems, video surveillance systems, robots, sensors, and wearable devices produces a huge amount of voice-data traffic in the near future. To meet the growth and to provide fast and ubiquitous Internet access, several promising technologies have been developed. Regarding the deployment of the 5G wireless communication systems, the corresponding growth in the demand for wireless radio spectrum resources will appear. The capacity of the communication networks will be increased by using the energy-efficiency techniques with the evolving technology in 5G networks [2–5].

One of the candidates for solving the problem of spectrum shortage is the CR network which will be a key technology for 5G networks. CR has attracted considerable interest as it can cope with the spectrum underutilization phenomenon. Performing spectrum sharing using a CR network is an important issue in wireless communication networks. There are three main ways for a primary network user to share the frequency spectrum with a cognitive user: underlay, overlay, and interweave. In the underlay method, the secondary user (SU) transmits its information simultaneously with the primary user (PU) as long as the interference between SU and PU receivers is within a predefined threshold. In the overlay approach, SU helps PU by sharing its resources, and in return, PU allows SU to communicate. In the interweave technique, SU can use the bandwidth of PU if PU is not active. In this model, SU should have perfect spectrum-sensing features to analyze the spectrum [6–9].

Among the various methods of solving the interference problem, interference alignment (IA) is one of the most promising ways to achieve it. IA is an important approach for CR to

http://dx.doi.org/10.5772/intechopen.80073

recover the desired signal by utilizing the precoding and linear suppression matrices which consolidates the interference beam into one subspace in order to eliminate it [10–13]. In the literature, linear IA is adopted in CR interference channels in [14–20] and the references therein. In [14], adaptive power allocation schemes are considered for linear IA-based CR networks where the outage probability and sum rate were derived. In [15], adaptive power allocation was studied for linear IA-based CR using antenna selection at the receiver side. Ref. [16] enhances the security of CR networks by using a zero-forcing precoder. Moreover, in [17], a similar work was proposed to improve the overall outage performance of the interference channel by using power allocation optimization. These studies have shown that interference management is a critical issue to be handled in all multiuser wireless networks.

CR technology can be capable of utilizing the spectrum efficiently as long as the interference between PU and SU is perfectly aligned as shown in **Figure 1**. A set of studies discussing IA is presented in the literature [21–29].

Motivated by the above works, in the first part of this study, we examine the impact of interference leakage on multi-input multi-output (MIMO) CR networks with multiple SUs. Specifically, a closed-form outage probability expression is derived to provide the performance of the primary system. Then, in the second part of our work, we investigate the performance of IA in underlay CR networks for Rayleigh fading channel. Moreover, unlike the mentioned papers, the effect of CSI quantization error is taken into account in our analysis. Then, a two-way relaying scheme with amplify-and-forward (AF) strategy is studied. Finally, the effects of the relay location and the path loss exponent on the BER performance and system capacity and CSI quantization on the average pairwise error probability (PEP) performance for this two-way AF system are presented.

The main simulation parameters and their descriptions used in this study are summarized in **Table 1**.

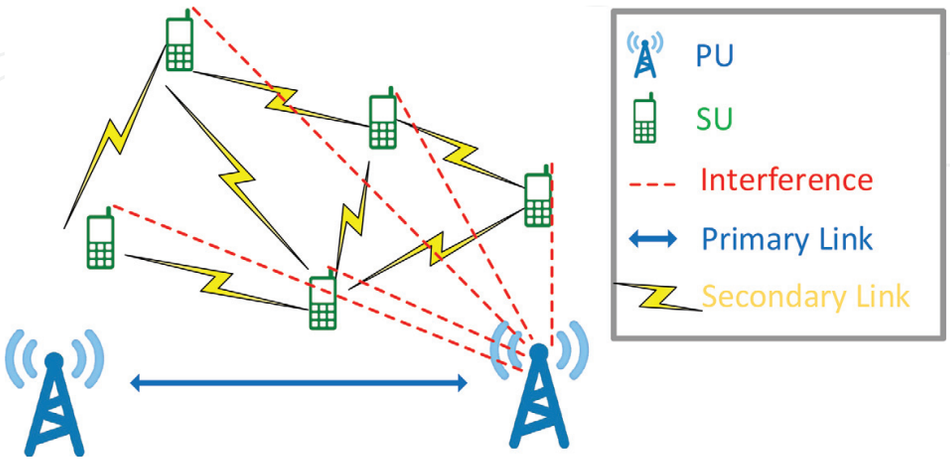

Figure 1. Illustration of the primary link between PU pair and interference links generated by the SUs.

Symbol	Description
P_1 and P_2	Transmitted powers of the PU and SU
σ_N^2	Variance of the circularly symmetric additive white Gaussian noise vector
R_{th}	Data rate threshold
α	Interference-leakage parameter
M_p and N_p	Number of transmit-and-receive antennas of PU
M_s and N_s	Number of transmit-and-receive antennas of SU
K	Number of SU
$d_{j,i}$	Distance between the ith transmitter and the jth receiver nodes
$\tau_{j,i}$	Path loss exponent between the ith transmitter and the jth receiver nodes
$B_{j,i}$	Channel state information exchange amount between the ith transmitter and the jth receiver nodes

Table 1. The simulation symbols and their descriptions.

2. The impact of interference leakage on MIMO CR networks

In this study, MIMO interference alignment-based CR network with a PU and multiple SUs is considered under Rayleigh fading channel.

2.1. System model

In the system model as it is shown in **Figure 2**, the number of transmit-and-receive antennas of the PU is given by M_p and N_p. The transmit antennas at each SU are given as M_s. The received signal, $\mathbf{y}_p$, implementing the IA technique is given as

$$\mathbf{y}_p = \mathbf{U}_p^{\mathrm{H}}\mathbf{H}_{pp}\mathbf{V}_p\mathbf{x}_p + \sqrt{\alpha}\sum_{i=1}^{K}\mathbf{U}_s^{\mathrm{H}}\mathbf{H}_{ps_i}\mathbf{V}_s\mathbf{x}_{s_i} + \mathbf{U}_p^{\mathrm{H}}\mathbf{n}, \tag{1}$$

where x_p and x_{s_i} are the transmitted signals from PU and the ith SU (for $i = 1, 2, \ldots, K$), respectively. Herein, $\mathbf{H}_{pp}$ is the matrix of channel coefficients between the PU pair, and $\mathbf{H}_{ps_i}$ denotes the channel matrix between the primary receiver and the ith secondary transmitter. The interference leakage is modeled similar to the one in [30]. The interference-leakage parameter α $(0 \le \alpha \le 1)$ represents the status of the alignment, i.e., $\alpha = 0$ and 1 corresponds to perfect alignment and perfect misalignment cases, respectively. $\mathbf{V}$ and $\mathbf{U}$ are the precoding- and interference-suppression matrices. The superscript $(\cdot)^{\mathrm{H}}$ denotes the Hermitian operator, and $\mathbf{n}$ is the zero-mean unit variance ($\sigma_N^2 = 1$) circularly symmetric additive white Gaussian noise (AWGN) vector.

The following conditions must be satisfied for perfect interference alignment between PU and SUs:

http://dx.doi.org/10.5772/intechopen.80073

$$\mathbf{U}_s^{\mathrm{H}}\mathbf{H}_{ps_i}\mathbf{V}_s\mathbf{x}_{s_i} = 0, \tag{2}$$

$$\mathrm{Rank}\left(\mathbf{U}_s^{\mathrm{H}}\mathbf{H}_{ps_i}\mathbf{V}_s\mathbf{x}_{s_i}\right) = d. \tag{3}$$

Each user transmits d data streams. Using the ideal linear IA technique, (1) can be re-expressed as

$$\mathbf{y}_p = \mathbf{U}_p^{\mathrm{H}}\mathbf{H}_{pp}\mathbf{V}_p\mathbf{x}_p + \mathbf{U}_p^{\mathrm{H}}\mathbf{n}. \tag{4}$$

2.2. Outage probability analysis

The channel capacity and outage probability are the most important impairments which affect the quality of service (QoS) in wireless communication systems. When no CSI conditions are

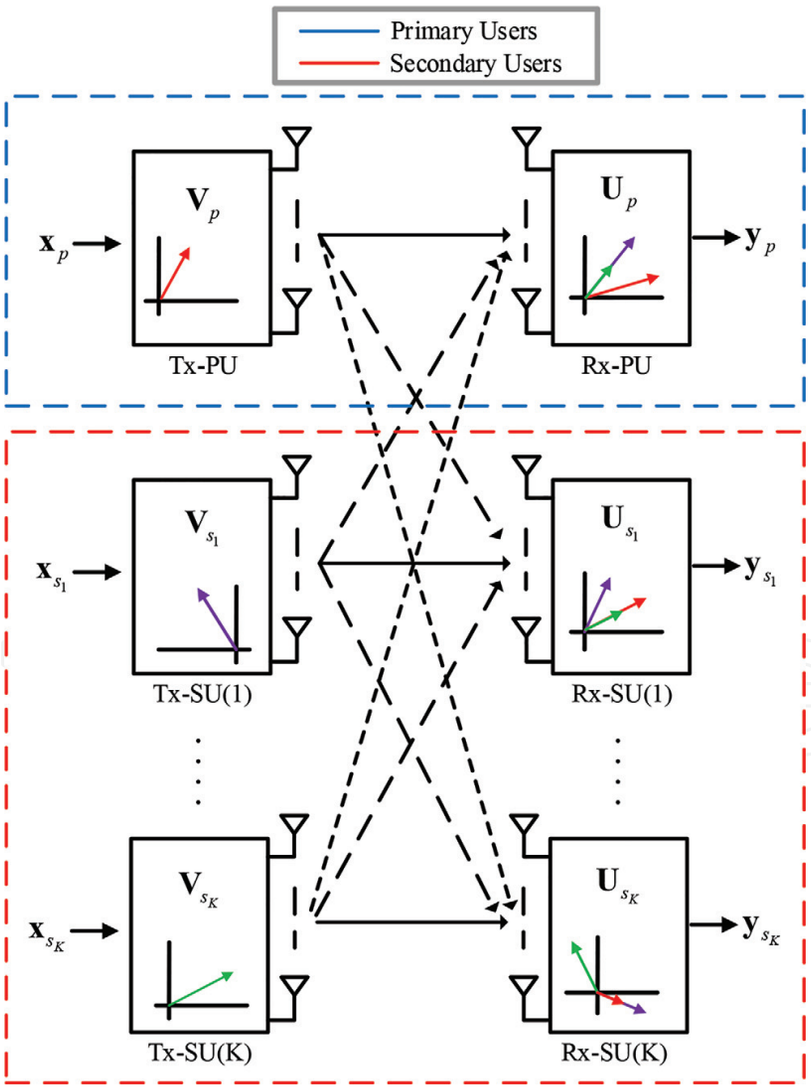

Figure 2. IA-based CR network with single PU and K SUs sharing the spectrum.

given, MIMO channel capacity is expressed as in [31]. The channel capacity of the considered MIMO system in PU can be expressed as

$$C = \log_2 \det\left|\mathbf{I} + \frac{\gamma_1}{(1+\gamma_2)N_p}\mathbf{H}_{pp}\mathbf{H}_{pp}^{H}\right|, \tag{5}$$

where $\gamma_1 = P_1\left\|\mathbf{H}_{pp}\right\|^2/\sigma_N^2$ is the signal-to-noise ratio (SNR) of the primary link. γ_2 can be expressed as $\gamma_2 = \left(P_2/\sigma_N^2\right)\sum_{i=1}^{K}\left\|\mathbf{H}_{ps_i}\right\|^2$. Note that $\|.\|^2$ demonstrates the squared Frobenius norm of the channel matrix, $\mathbf{I}$ denotes for identity matrix, and P_1 and P_2 are the transmitted powers of the PU and SUs, respectively. If linear IA perfectly eliminates the interference between SU and PU, then SNR of the interference channel, γ_2, becomes zero. It is important to note that precoding and linear suppression vectors are assumed as $\left|\mathbf{U}_p^{\mathrm{H}}\right|^2 = \left|\mathbf{V}_p\right|^2 = \left|\mathbf{U}_{s_i}^{\mathrm{H}}\right|^2 = \left|\mathbf{V}_{s_i}\right|^2 = 1$. In the presence of interference-free communication, primary system works in the single-input and single-output (SISO) fashion [14]. Hence, the probability density function (PDF) of γ_1 can be written as $f_{\gamma_1}(\gamma) = \frac{1}{\overline{\gamma}_1}\exp\left(-\gamma/\overline{\gamma}_1\right)$, and the outage probability of the system can be obtained as

$$P_{out} = \int_0^{2^{R_{th}}-1} f_{\gamma_1}(\gamma)d\gamma, \tag{6}$$

where R_{th} is the data rate threshold and $\overline{\gamma}_1 = P_1/\sigma_N^2$ denotes the average SNR of the primary system. By substituting $f_{\gamma_1}(\gamma)$ into (6), the outage probability can be obtained as

$$P_{out} = 1 - \exp\left(\frac{2^{R_{th}}-1}{\overline{\gamma}_1}\right). \tag{7}$$

In the presence of interference, the primary system works in MIMO fashion, and leakages may occur due to fast-fading Rayleigh channel. To improve the performance of the primary system, we adopt maximum ratio transmission and maximum ratio combining at the transmitter and receiver, respectively. Thereby, the end-to-end signal-to-interference-plus-noise ratio (SINR) of the primary system can be written as $\gamma_\tau = \gamma_1/(1+\gamma_2)$. In the proposed system, all channels are modeled as independent and identically distributed Chi-squared distribution, and the PDF of γ_1 can be expressed as

$$f_{\gamma_1}(\gamma) = \frac{\gamma^{M_pN_p-1}\exp\left(-\gamma/\left(\overline{\gamma}_1/M_p\right)\right)}{\left(\frac{\overline{\gamma}_1}{M_p}\right)^{M_pN_p}\left(M_pN_p-1\right)!}. \tag{8}$$

In addition, the PDF of γ_2 can be defined as

$$f_{\gamma_2}(\gamma) = \frac{\gamma^{KM_sN_p-1}\exp\left(-\gamma/\left(\alpha\overline{\gamma}_2/M_s\right)\right)}{\left(\frac{\alpha\overline{\gamma}_2}{M_s}\right)^{KM_sN_p}\left(KM_sN_p-1\right)!}, \tag{9}$$

where $\overline{\gamma}_2 = P_2/\sigma_N^2$ is the average SNR of the secondary system. Finally, the PDF of γ_τ can be written as

$$f_{\gamma_\tau}(\gamma) = \int_0^\infty (x+1) f_{\gamma_1}((x+1)\gamma) f_{\gamma_2}(x) dx. \tag{10}$$

By substituting (8) and (9) into (10), then with the help of [32, Eq. 3.351.3] and after few manipulations, PDF expression of $f_{\gamma_\tau}(\gamma)$ is given as

$$f_{\gamma_\tau}(\gamma) = \Delta \sum_{m=0}^{M_p N_p} \binom{M_p N_p}{m} (KM_s N_p + m - 1)! \left(\frac{\gamma M_p}{\overline{\gamma}_1} + \frac{M_s}{\alpha \overline{\gamma}_2}\right)^{-KM_s N_p + m}. \tag{11}$$

Furthermore, collecting constant terms in (11), Δ is defined by

$$\Delta = \beta \gamma^{M_p N_p - 1} \exp\left(-\frac{M_p \gamma}{\overline{\gamma}_1}\right). \tag{12}$$

Hereby, β is constituted as

$$\beta = \frac{\left(\frac{\overline{\gamma}_1}{M_p}\right)^{-M_p N_p} \left(\frac{\alpha \overline{\gamma}_2}{M_s}\right)^{-KM_s N_p}}{(M_p N_p - 1)!(KM_s N_p - 1)!}. \tag{13}$$

To achieve the closed-form expression of (11), binomial expression of $\left(\frac{\gamma M_p}{\overline{\gamma}_1} + \frac{M_s}{\alpha \overline{\gamma}_2}\right)^{-KM_s N_p + m}$ term must be completed. The binomial expansion of this negative exponential term is given as

$$\left(\frac{\gamma M_p}{\overline{\gamma}_1} + \frac{M_s}{\alpha \overline{\gamma}_2}\right)^{-\zeta} = \sum_{t=0}^{\infty} (-1)^t \binom{\zeta + t - 1}{t} \left(\frac{\gamma M_p}{\overline{\gamma}_1}\right)^t \left(\frac{Ms}{\alpha \overline{\gamma}_2}\right)^{\zeta + t}, \tag{14}$$

where ζ is given as $\zeta = KM_s N_p + m$. Besides, the validation of (14) is restricted via $|\frac{\gamma M_p}{\overline{\gamma}_1}| < \frac{M_s}{\alpha \overline{\gamma}_2}$ condition. Under these conditions, the closed-form expression of f_{γ_τ} is given below:

$$f_{\gamma_\tau}(\gamma) = \Delta \sum_{m=0}^{M_p N_p} \sum_{t=0}^{\infty} (-1)^t \binom{M_p N_p}{m} (\zeta - 1)! \binom{\zeta + t - 1}{t} \left(\frac{\gamma M_p}{\overline{\gamma}_1}\right)^t \left(\frac{Ms}{\alpha \overline{\gamma}_2}\right)^{\zeta + t}. \tag{15}$$

Outage probability function of the proposed MIMO system with respect to f_{γ_τ} can be expressed as

$$P_{out} = \int_0^{2^{R_{th}} - 1} f_{\gamma_\tau}(\gamma) d\gamma. \tag{16}$$

The closed-form expression for (16) can be validated with the numerical integral operation [33].

2.3. Performance evaluation

Herein, the system performance of the MIMO CR network is studied in the presence of interference leakage for Rayleigh fading channel by comparing the analytical results with computer simulations. We assumed $P_1 = P_2 = \rho$ while $\sigma_N^2 = 1$ in the performance evaluation.

In **Figure 3**, the P_{out} performance for different R_{th} values is presented. We take $\alpha = -20$ dB, $M_p = 2$, $N_p = 2$, $K = 5$, and $M_s = 1$. It can be seen from **Figure** 3 that when R_{th} is increased from 1 to 4 bits/channel, the P_{out} performance is degraded.

In **Figure 4**, the impact of the leakage coefficient, α, on the outage probability performance is depicted for $M_p = 2$, $N_p = 2$, $K = 1$, $M_s = 1$, and $R_{th} = 3$ bits/channel. As can be seen from the figure, when α is changed from -10 dB to -30 dB, the performance of the primary system is enhanced.

In **Figure 5**, α, M_p, N_p, M_s, and R_{th} are taken as -20 dB, 2, 2, 1, and 1 bits/channel, respectively. It can be observed from the figure that increasing the number of SUs decreases the outage probability performance of the primary system considerably.

In **Figure 6**, the impact of antenna diversity on the P_{out} performance is investigated for $\alpha = -10$ dB, $K = 2$, and $R_{th} = 1$ dB. It is observed from the figure that, when the number of antennas at the primary transmitter and receiver increases, the system performance enhances. Besides, the receiver diversity effect on the system performance is greater than the transmitter diversity, as expected.

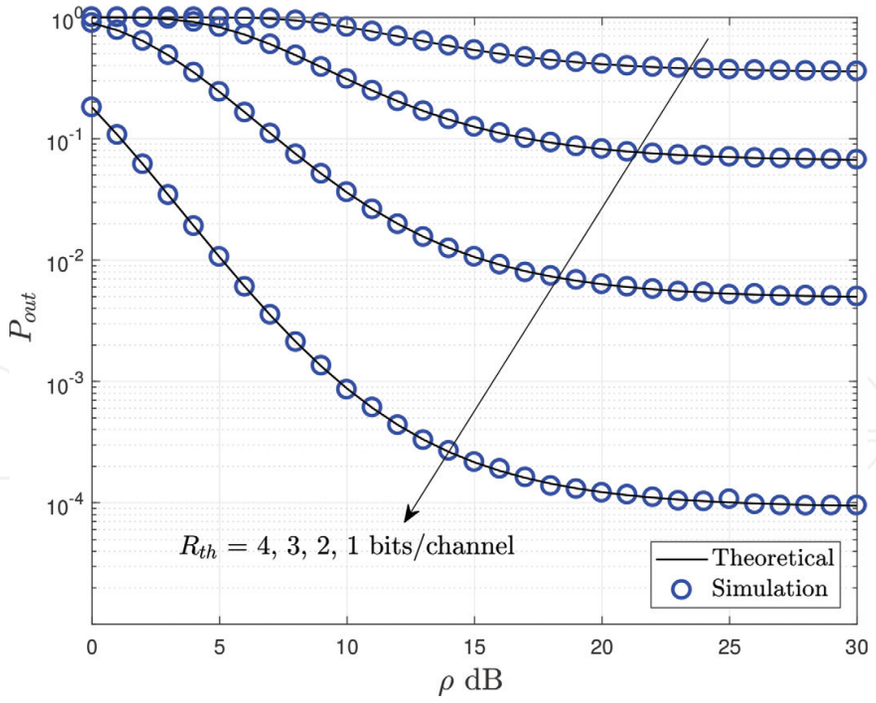

Figure 3. P_{out} performance for different data rate threshold R_{th}.

http://dx.doi.org/10.5772/intechopen.80073

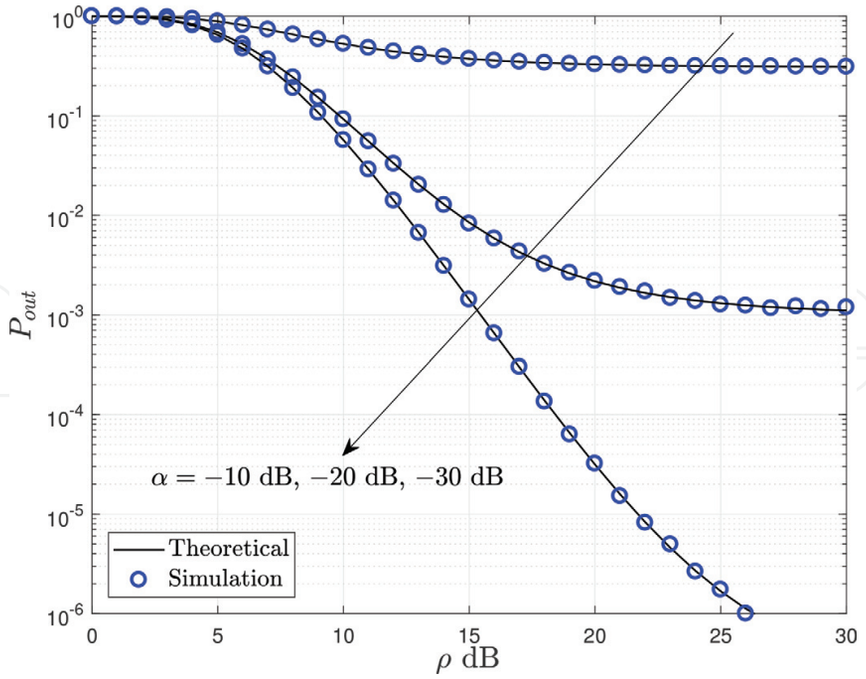

Figure 4. P_{out} performance with varying SNR for different interference-leakage values.

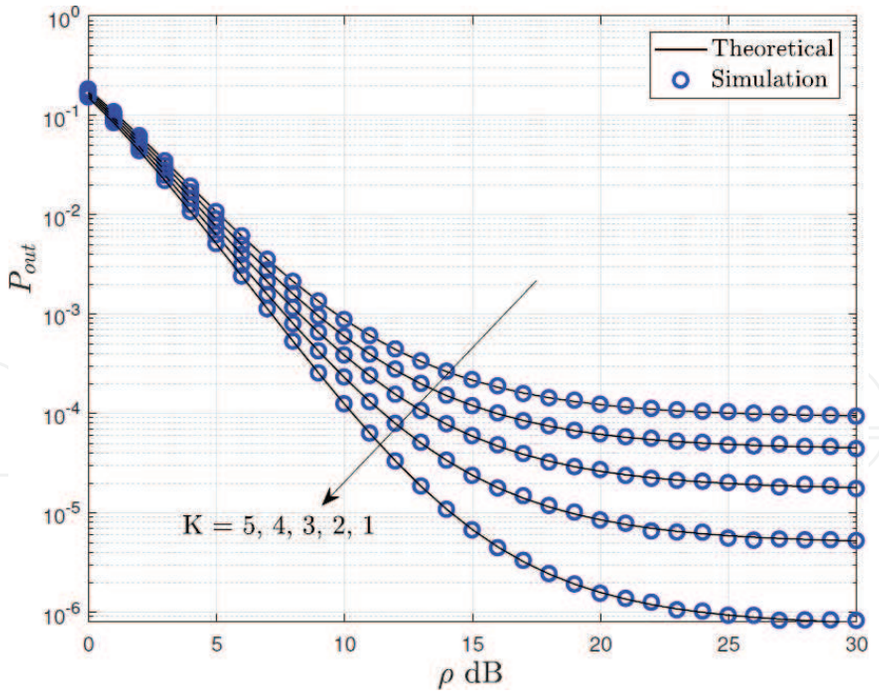

Figure 5. P_{out} vs. SNR for different numbers of SUs.

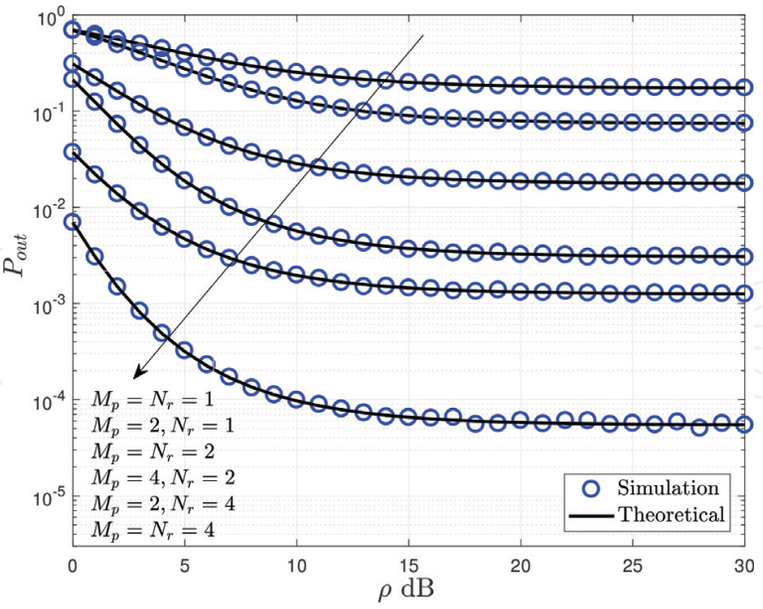

Figure 6. The effect of antenna diversity on the outage probability performance.

3. The effect of CSI quantization on interference alignment in CR networks

In this section, we investigate a cognitive two-way relaying network composed of a primary network (PN) with one pair of PU and a secondary network (SN) with two source terminals and a relay terminal (R).

3.1. System model

We consider a MIMO interference network shown in **Figure 7**, where the transmitter, T_x, and receiver, R_x, are equipped with M_1 and N_1 antennas in PN, respectively. Each PN transmitter transmits to its corresponding receiver by interfering with the SN nodes, namely, two source terminals (S_1 and S_2) and a relay terminal. That means T_x transmitter sends messages to its intended receiver R_x, whereas it also causes interference to the unintended receivers in the SN. The SN consists of two source terminals and a relay terminal. We assume that all nodes in SN operate in an AF half-duplex mode with the help of information relaying from each source terminal to R in two phases. All nodes in SN are assumed to have MIMO antennas, and there is no direct transmission between S_1 and S_2 [34–36]. We consider a scenario where the source terminals and a relay terminal are equipped with N_{S_1}, N_{S_2}, and N_R antennas, respectively. In the system model based on IA for cognitive two-way relay network, the received signal at R_x in PN can be written as

$$\mathbf{y}_{R_x} = \sqrt{\frac{P_{T_x}}{d_{R_x,T_x}^{\tau_{R_x,T_x}}}}\mathbf{U}_{R_x}^H \mathbf{H}_{R_x,T_x}\mathbf{V}_{T_x}\mathbf{s}_{T_x} + \boldsymbol{r} + \tilde{\mathbf{n}}_{R_x}, \tag{17}$$

http://dx.doi.org/10.5772/intechopen.80073

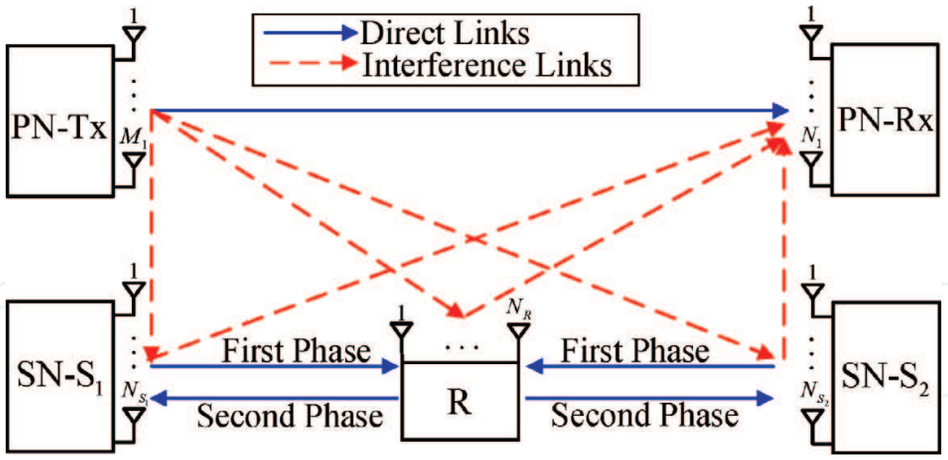

Figure 7. System model for interference alignment-based cognitive two-way relay network with primary network and secondary network.

where Υ is the interference term generated from SN to R_x defined as follows:

$$\Upsilon = \begin{cases} \sqrt{\frac{P_{S_1}}{d_{R_x,S_1}^{\tau_{R_x,S_1}}}}\mathbf{U}_{R_x}^H \mathbf{H}_{R_x,S_1}\mathbf{V}_{S_1}\mathbf{s}_{S_1} + \sqrt{\frac{P_{S_2}}{d_{R_x,S_2}^{\tau_{R_x,S_2}}}}\mathbf{U}_{R_x}^H \mathbf{H}_{R_x,S_2}\mathbf{V}_{S_2}\mathbf{s}_{S_2}, & \text{first phase} \\ \sqrt{\frac{P_R}{d_{R_x,R}^{\tau_{R_x,R}}}}\mathbf{U}_{R_x}^H \mathbf{H}_{R_x,R}\mathbf{V}_R\mathbf{s}_R, & \text{second phase.} \end{cases} \tag{18}$$

The effective additive white Gaussian noise (AWGN) term with zero mean and unit variance, $\tilde{\mathbf{n}}_{R_x}$ at R_x in PN, is defined by $\mathbf{U}_{R_x}^H \mathbf{n}_{R_x}$, where $\mathbf{n}_{R_x}$ is the AWGN vector with $\mathrm{E}\left[\mathbf{n}_{R_x}\mathbf{n}_{R_x}^H\right] = \sigma_{R_x}^2\mathbf{I}$ in which $\mathbf{I}$ is the unitary matrix, $\sigma_{R_x}^2$ is the noise variance, and E[.] is the expectation operator. The transmit powers at the terminals T_x, S_1, S_2, and R are denoted by P_i, for $i = T_x$, S_1, S_2, and R, respectively. Each receive node employs the interference-suppression matrix, $\mathbf{U}_j$, (for $j = R_x$, R, S_1, S_2), while each transmit node employs a precoding matrix $\mathbf{V}_i$ [37]. The conjugate transpose of the matrix is associated with the Hermitian operator $(.)^H$ [38]. The transmit signal vector for the ith user is defined by $\mathbf{s}_i$. The channel between the ith transmitter and the jth receiver nodes is denoted by $\mathbf{H}_{j,i}$ for both PN and SN. The quantized CSI is passed to the transmitter by the corresponding receiver. Because of limited feedback, the transmitters have imperfect CSI causing certain performance loss. To clarify the effect of CSI quantization error on the performance of interference alignment in underlay cognitive two-way relay networks, we investigate the BER performance, instantaneous capacity, and average PEP of the considered system. Based upon the accuracy parameter, the relation between perfect CSI ($\rho_{j,i} = 0$) and imperfect CSI ($0 < \rho_{j,i} \leq 1$) can be given as

$$\mathbf{H}_{j,i} = \sqrt{1-\rho_{j,i}}\hat{\mathbf{H}}_{j,i} + \sqrt{\rho_{j,i}}\mathbf{E}_{j,i}, \tag{19}$$

where $\mathbf{H}_{j,i}$ is the real channel matrix and $\hat{\mathbf{H}}_{j,i}$ is the estimated channel matrix. The quantization error, $\mathbf{E}_{j,i}1mm$, can be expressed with the upper bound of $2^{-B_{j,i}/(M_1N_1-1)}$, where $B_{j,i}$ is the CSI

exchange amount and M_1 and N_1 are the numbers of transmit-and-receive antennas, successively [21, 39]. It is assumed that both $\hat{\mathbf{H}}_{j,i}$ and $\mathbf{E}_{j,i}$ are independent of $\mathbf{H}_{j,i}$. Besides, each channel link is also modeled by two additional parameters: the distance between ith transmitter and the jth receiver nodes $d_{j,i}$ and the path loss exponent for the corresponding link, $\tau_{j,i}$, regarding for different radio environments, respectively.

In the first phase of the transmission (multiple-access phase) in SN, both S_1 and S_2 transmit their signals simultaneously to the relay terminal, R. Then the received signal at R can be written as

$$\mathbf{y}_R = \sqrt{\frac{P_{S_1}}{d_{R,S_1}^{\tau_{R,S_1}}}}\mathbf{U}_R^H\mathbf{H}_{R,S_1}\mathbf{V}_{S_1}\mathbf{s}_{S_1} + \sqrt{\frac{P_{S_2}}{d_{R_x,S_2}^{\tau_{R_x,S_2}}}}\mathbf{U}_R^H\mathbf{H}_{R,S_2}\mathbf{V}_{S_2}\mathbf{s}_{S_2} + \sqrt{\frac{P_{T_x}}{d_{R,T_x}^{\tau_{R,T_x}}}}\mathbf{U}_R^H\mathbf{H}_{R,T_x}\mathbf{V}_{T_x}\mathbf{s}_{T_x} + \tilde{\mathbf{n}}_R, \quad (20)$$

where $\tilde{\mathbf{n}}_R = \mathbf{U}_R^H\mathbf{n}_R$ at the relay terminal in SN is expressed as zero-mean AWGN vector with $\mathrm{E}\left[\mathbf{n}_R\mathbf{n}_R^H\right] = \sigma_R^2\mathbf{I}$ in which the noise variance at the relay terminal is depicted with σ_R^2. Besides, the received signal at S_1 and S_2 terminals in SN is defined, respectively, as

$$\mathbf{y}_{S_1} = \sqrt{\frac{P_R}{d_{S_1,R}^{\tau_{S_1,R}}}}\mathbf{U}_{S_1}^H\mathbf{H}_{S_1,R}\mathbf{V}_R\mathbf{s}_R + \sqrt{\frac{P_{T_x}}{d_{S_1,T_x}^{\tau_{S_1,T_x}}}}\mathbf{U}_{S_1}^H\mathbf{H}_{S_1,T_x}\mathbf{V}_{T_x}\mathbf{s}_{T_x} + \tilde{\mathbf{n}}_{S_1}, \quad (21)$$

$$\mathbf{y}_{S_2} = \sqrt{\frac{P_R}{d_{S_2,R}^{\tau_{S_2,R}}}}\mathbf{U}_{S_2}^H\mathbf{H}_{S_2,R}\mathbf{V}_R\mathbf{s}_R + \sqrt{\frac{P_{T_x}}{d_{S_2,T_x}^{\tau_{S_2,T_x}}}}\mathbf{U}_{S_2}^H\mathbf{H}_{S_2,T_x}\mathbf{V}_{T_x}\mathbf{s}_{T_x} + \tilde{\mathbf{n}}_{S_2}. \quad (22)$$

Here, $\tilde{\mathbf{n}}_{S_1}$ and $\tilde{\mathbf{n}}_{S_2}$ are the AWGN vector with $\mathrm{E}\left[\mathbf{n}_{S_k}\mathbf{n}_{S_k}^H\right] = \sigma_{S_k}^2\mathbf{I}$, for $k = 1, 2$ and the noise variance of $\sigma_{S_k}^2$. In addition to that, in the second phase of the signal transmission (broadcast phase), R broadcasts the combined signal $\mathbf{y}_R$ after multiplying with an ideal amplifying gain, G, which is expressed as

$$G = 1/\sqrt{\frac{P_{S_1}(1-\rho_{R,S_1})}{d_{R,S_1}^{\tau_{R,S_1}}}\|\mathbf{U}_R^H\hat{\mathbf{H}}_{R,S_1}\mathbf{V}_{S_1}\|^2 + \frac{P_{S_2}(1-\rho_{R,S_2})}{d_{R,S_2}^{\tau_{R,S_2}}}\|\mathbf{U}_R^H\hat{\mathbf{H}}_{R,S_2}\mathbf{V}_{S_2}\|^2 .. + \frac{P_{T_x}(1-\rho_{R,T_x})}{d_{R,T_x}^{\tau_{R,T_x}}}\|\mathbf{U}_R^H\hat{\mathbf{H}}_{R,T_x}\mathbf{V}_{T_x}\|^2}}, \quad (23)$$

where $\mathbf{s_R} = G\mathbf{y}_R$. We assume that both S_1 and S_2 have knowledge about their own information and can remove back-propagating self-interference from the imposed signals. We also assume that all interference at the receive terminals are perfectly aligned and the following feasible conditions are satisfied for the receive nodes:

$$\mathbf{U}_j^{\mathrm{H}}\mathbf{H}_{j,i}\mathbf{V}_i\mathbf{s}_i = 0, \quad (24)$$

$$\mathrm{rank}\left(\mathbf{U}_j^{\mathrm{H}}\mathbf{H}_{j,i}\mathbf{V}_i\mathbf{s}_i\right) = f_i, \quad (25)$$

where f_i is the degree of freedom and rank (.) denotes the rank operation of a matrix. By assuming that the interference is perfectly aligned by the proposed IA algorithm, and the

channel matrices are constant during the transmission, we ensure that there is no interference from the unintended transmitters and guarantee that received signal achieves f_i degrees of freedom [39]. The corresponding signal-to-interference-plus-noise ratio (SINR) for the links $T_x \rightarrow R_x$, $S_1 \rightarrow R$, and $R \rightarrow S_2$ can be derived by

$$\gamma_{T_x \rightarrow R_x} = \frac{\frac{P_{T_x}\left(1-\rho_{R_x,T_x}\right)}{d_{R_x,T_x}^{\tau_{R_x,T_x}}} \|\mathbf{U}_{R_x}^H \hat{\mathbf{H}}_{R_x,T_x} \mathbf{V}_{T_x}\|^2}{\Psi + \sigma_{\tilde{n}_{R_x}{}^2}}, \tag{26}$$

$$\gamma_{S_1 \rightarrow R} = \frac{\frac{P_{S_1}\left(1-\rho_{R,S_1}\right)}{d_{R,S_1}^{\tau_{R,S_1}}} \|\mathbf{U}_R^H \hat{\mathbf{H}}_{R,S_1} \mathbf{V}_{S_1} \mathbf{s}_{S_1}\|^2}{\frac{P_{T_x}\rho_{R,T_x}}{d_{R,T_x}^{\tau_{R,T_x}}} \|\mathbf{U}_R^H \mathbf{E}_{R,T_x} \mathbf{V}_{T_x}\|^2 + \sigma_{\tilde{n}_R}^2}, \tag{27}$$

$$\gamma_{R \rightarrow S_2} = \frac{\frac{P_R\left(1-\rho_{S_2,R}\right)}{d_{S_2,R}^{\tau_{S_2,R}}} \|\mathbf{U}_{S_2}^H \hat{\mathbf{H}}_{S_2,R} \mathbf{V}_R \mathbf{s}_R\|^2}{\frac{P_{T_x}\rho_{S_2,T_x}}{d_{S_2,T_x}^{\tau_{S_2,T_x}}} \|\mathbf{U}_{S_2}^H \mathbf{E}_{S_2,T_x} \mathbf{V}_{T_x}\|^2 + \sigma_{\tilde{n}_{S_2}}^2}, \tag{28}$$

$$\Psi = \begin{cases} \frac{P_{S_1}\rho_{R_x,S_1}}{d_{R_x,S_1}^{\tau_{R_x,S_1}}} \|\mathbf{U}_{R_x}^H \mathbf{E}_{R_x,S_1} \mathbf{V}_{S_1}\|^2 + \frac{P_{S_2}\rho_{R_x,S_2}}{d_{R_x,S_2}^{\tau_{R_x,S_2}}} \|\mathbf{U}_{R_x}^H \mathbf{E}_{R_x,S_2} \mathbf{V}_{S_2}\|^2, & \text{first phase} \\ \frac{P_R \rho_{R_x,R}}{d_{R_x,R}^{\tau_{R_x,R}}} \|\mathbf{U}_{R_x}^H \mathbf{E}_{R_x,R} \mathbf{V}_R\|^2, & \text{second phase} \end{cases} \tag{29}$$

where $\mathbf{E}_{j,i}$ is the quantization error and $\|.\|$ is the Euclidean norm. In here, $\gamma_{S_2 \rightarrow R}$ and $\gamma_{R \rightarrow S_1}$ can be found by changing the subscript S_1 with S_2 of (27) and S_2 with S_1 of (28). Assuming the channels are reciprocal over SN direct links, thus the channel gains for $S_1 \rightarrow R$ and $R \rightarrow S_1$ and $S_2 \rightarrow R$ and $R \rightarrow S_2$ links are identical, respectively.

3.2. Performance analysis

This section starts by the instantaneous capacity analysis of the proposed system with interference alignment in underlay cognitive two-way relay networks with CSI quantization. We then study the BER and average PEP performance.

The capacity is expressed as the expected value of the mutual information between the transmitting terminal and receiving one. In light of this fact, we consider the method developed in [29]; the instantaneous capacity in PN can be expressed as

$$C_{R_x} = \log_2\left(1 + \gamma_{T_x \rightarrow R_x}\right), \tag{30}$$

where $\gamma_{T_x \rightarrow R_x}$ is the instantaneous SINR for the corresponding link of $T_x \rightarrow R_x$. On the other hand, end-to-end capacity for the SN, based on the least strong link over two-hop transmission, is denoted as follows:

$$C_R = \frac{1}{2}\log_2\left(1+\min\left(\gamma_{S_1\to R},\gamma_{R\to S_2}\right)\right)+\frac{1}{2}\log_2\left(1+\min\left(\gamma_{S_2\to R},\gamma_{R\to S_1}\right)\right). \tag{31}$$

$\gamma_{S_1\to R}$ and $\gamma_{R\to S_2}$ are the instantaneous SINR for the $S_1 \to R$ and $R \to S_2$ links, respectively.

Average BER for binary phase shift keying (BPSK) modulation can be expressed as

$$\mathrm{BER}_j = Q\left(\sqrt{\gamma_j}\right) \tag{32}$$

where $Q(x)$ is the Gaussian Q-function and defined by $Q(x) = \left(1/\sqrt{2\pi}\right)\int_x^\infty e^{-t^2/2}dt$ [37].

Average pairwise error probability ($\overline{\mathrm{PEP}}$) can be computed as averaging the Gaussian Q-function over Rayleigh fading statistics [40], $f_{\gamma_{T_x\to R_x}}(\gamma) = \left(e^{-\gamma/\overline{\gamma}_{T_x\to R_x}}\right)/\overline{\gamma}_{T_x\to R_x} 1mm$, where $\overline{\gamma}_{T_x\to R_x} = P_{T_x}\left(1-\rho_{R_x,T_x}\right)/d_{R_x,T_x}^{\tau_{R_x,T_x}}\sigma_{\tilde{n}_{R_x}}^2$

$$\overline{\mathrm{PEP}} = \int_0^\infty Q\left(\sqrt{\gamma_{T_x\to R_x}}\right) f_{\gamma_{T_x\to R_x}}(\gamma)d\gamma. \tag{33}$$

Finally, this integral can be evaluated with the help of Mathematica and average PEP under Rayleigh fading channel can be derived in a closed form as follows:

$$\overline{\mathrm{PEP}} = \frac{1}{2}\left(1-\sqrt{\frac{\overline{\gamma}_{T_x\to R_x}}{2+\overline{\gamma}_{T_x\to R_x}}}\right). \tag{34}$$

3.3. Numerical results

In this section the numerical results are provided with various scenarios to evaluate the performance analysis for IA in underlay cognitive two-way relay networks with CSI quantization. BER performance for direct transmission links of the proposed system is illustrated in **Figure 8** over Rayleigh distribution for different amounts of CSI exchange with varying SNR. For convenience, we set $d_{j,i} = 3\ m$ and $\tau = 2.7$, and 3×3 MIMO configuration is studied in this figure. Because of the number of interfering links, the quantization error for the $T_x \to R_x$ transmission is greater than the other links ($S_1 \rightleftarrows R \rightleftarrows S_2$). Even if the analyzed BER performance of the SN seems better than the PN, it should not be forgotten that SN operates in half-duplex mode. Performance loss in BER due to imperfect CSI ($B_{j,i} = 4$, for instance) becomes larger as SNR increases compared to the perfect CSI (for $B_{j,i} = \infty$) case.

In **Figure 9**, the average PEP versus SNR is plotted for $d_{j,i} = 3\ m$ and $\tau = 2.7$ over Rayleigh fading channel in PN. It can be noticed from the figure that as SNR increases, average PEP decreases, as expected. To reach the perfect CSI case, we take $B_{j,i} = \infty$, and the average PEP performance noticeably enhances. We also consider the case of imperfect CSI ($B_{j,i} = 4$) for the comparison purposes in the same figure.

http://dx.doi.org/10.5772/intechopen.80073

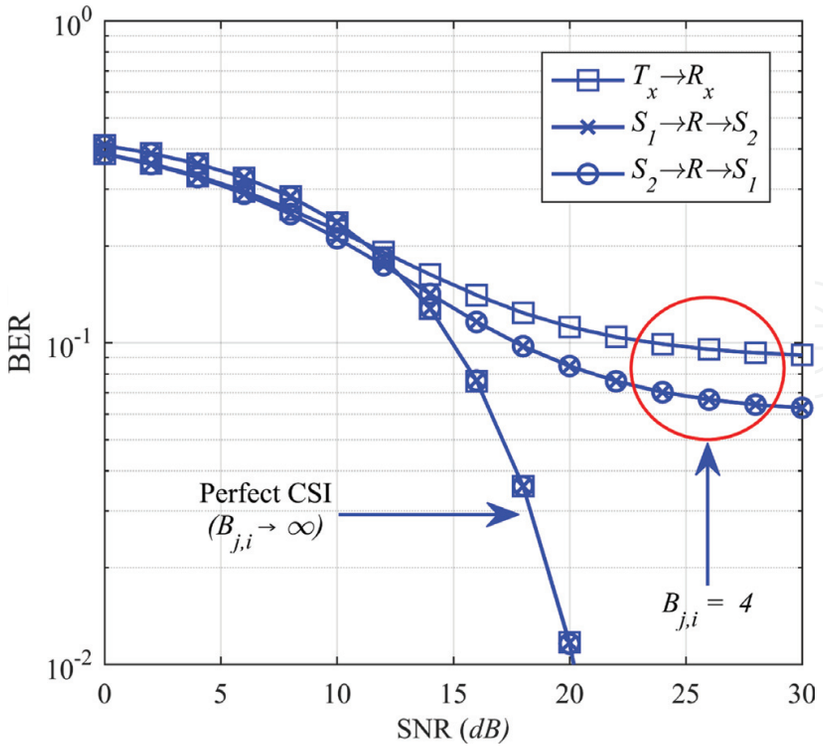

Figure 8. BER performance for different amounts of CSI exchange with varying SNR.

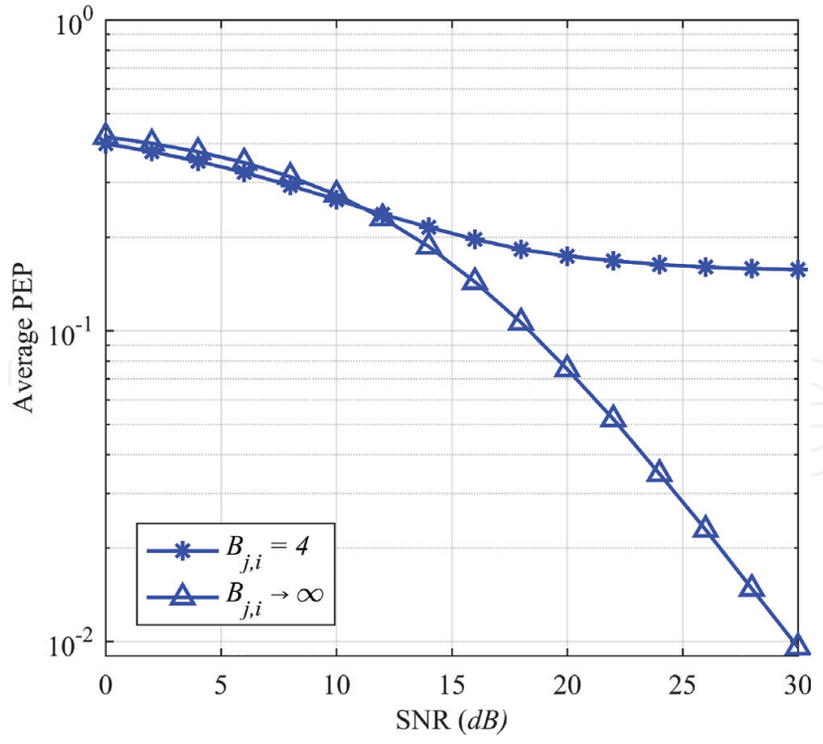

Figure 9. Average PEP performance for different amounts of CSI exchange with varying SNR over Rayleigh fading channel in primary network.

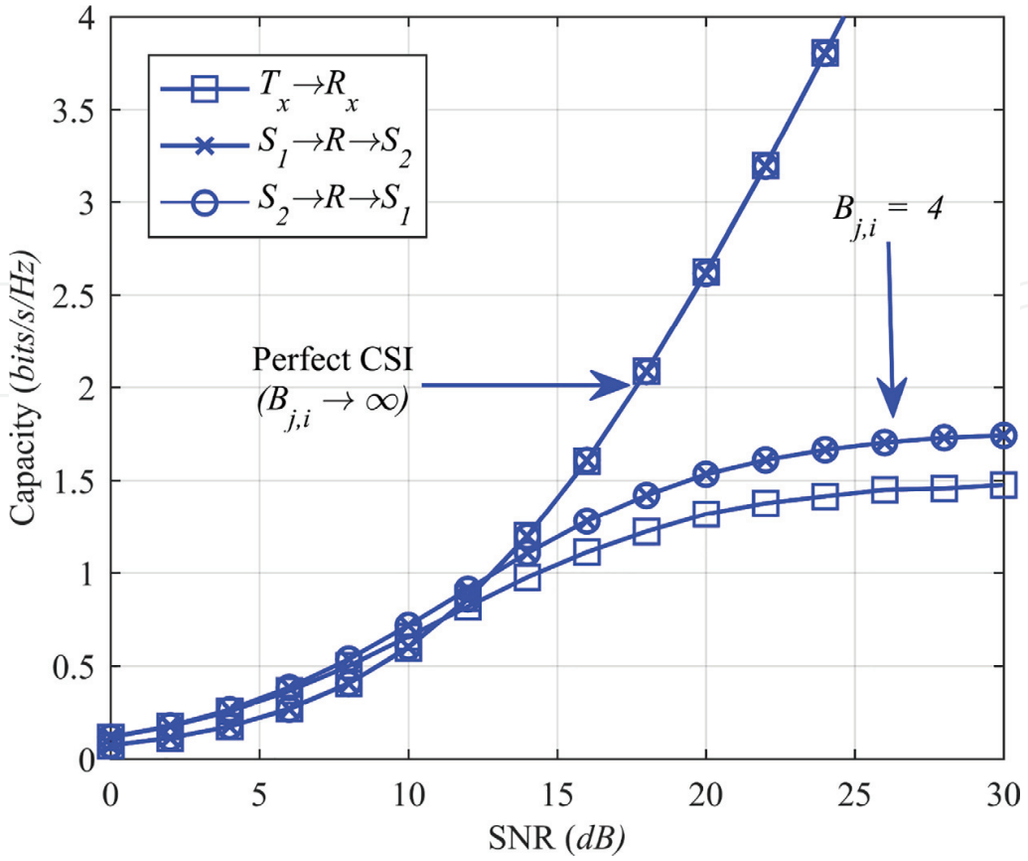

Figure 10. Capacity vs. SNR of the primary network and secondary network nodes under different CSI scenarios.

Figure 10 examines the capacity analysis with perfect and imperfect CSI for different direct links in PN and SN. The results clearly show that, examining the capacity with perfect CSI, performance improvement becomes larger as the SNR increases.

Figure 11 demonstrates the effects of $B_{j,i}$ and $d_{j,i}$ parameters on the BER performance for the SN with varying SNR when $\tau = 2.7$ and 3×3 MIMO scheme is used. The results clearly show that for a fixed SNR value, the performance of the considered system increases with the decrease of the $d_{j,i}$. It can be seen from the same figure that the increase on the amount of CSI exchange $B_{j,i}$ positively affects the BER performance.

Figure 12 shows the capacity performance of PU in the underlay cognitive two-way relay network over Rayleigh fading channel with varying path loss exponent, τ. The results show a performance improvement while the value of τ decreases. In this plot, $B_{j,i} = 8$, $d_{j,i} = 3$ m, and the 3×3 MIMO scheme are considered. Depending on the environmental conditions for mobile communications, typical τ values, ranging from 1.6 to 5, are used to plot this figure. First, for the line of sight in a building, the environment is considered with the τ values of 1.6 and 1.8. Second, capacity is computed for the free-space environment with $\tau = 2$. Then, the capacity performance is presented with τ values of 2.7 and 3.3 for urban area cellular radio environment. Finally, the shadowed urban cellular radio environment is associated with two different τ values of 3 and 5 to analyze the capacity performance with varying SNR [41].

http://dx.doi.org/10.5772/intechopen.80073

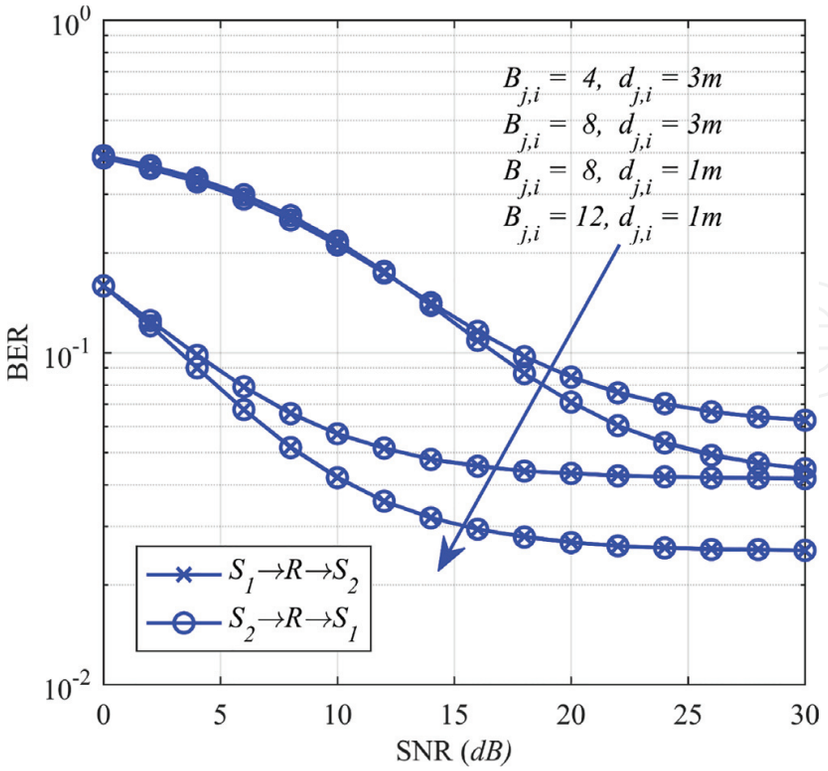

Figure 11. BER performance for different amounts of CSI exchange and distances with varying SNR over Rayleigh fading channel for secondary network.

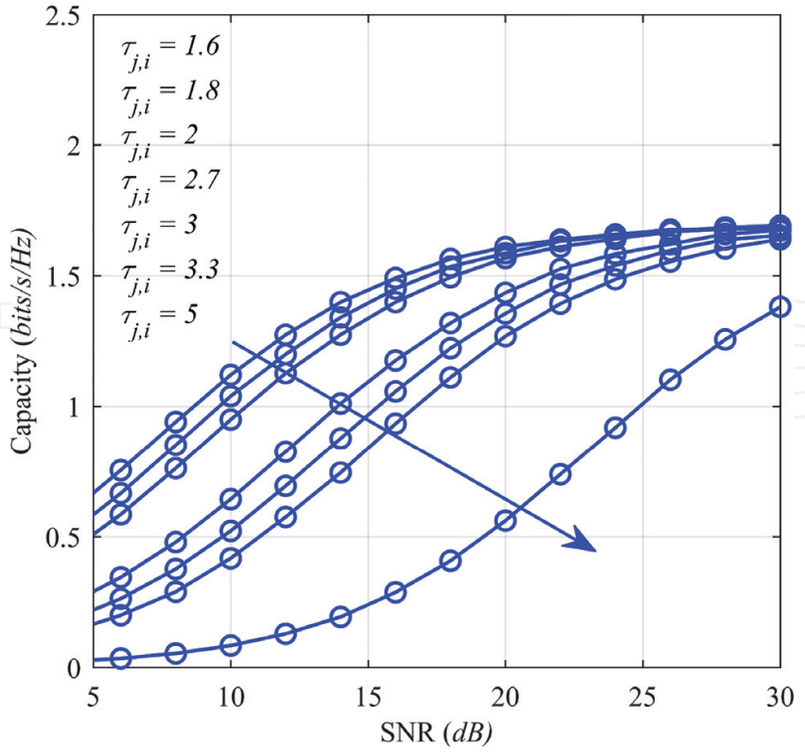

Figure 12. Capacity changes with SNR for the environmental conditions having different path loss exponents.

4. Conclusion

In this chapter, the system performance of linear interference alignment on the MIMO CR network is investigated under interference leakage. To quantify the performance of the primary system under a certain level of interference leakage, the closed-form outage probability expression is derived for Rayleigh fading channel. In all analyses, the theoretical results closely match with the simulations which confirm the accuracy of the derived expressions.

In the second part of this work, considering a practical issue, we investigate the performance of interference alignment in underlay cognitive radio network with CSI quantization error over general MIMO interference channel. Amplify-and-forward scheme for two-way relay network under Rayleigh fading is considered. The impact of the CSI exchange amount, the distance between the *i*th transmitter and the *j*th receiver nodes, and the path loss exponent on the BER performance, system capacity, and average PEP for the proposed system model are analyzed. We provide the exact closed-form expression for the average PEP in primary network over Rayleigh distribution, while IA algorithm perfectly eliminates the interference. The present performance analysis can be extended to the multiple secondary user pairs, and this approach will be another subject of our future work.

It would be interesting to study on various scenarios, including single-hop, multi-hop, and multi-way networks in future work to analyze the system performance over the recently developed interference alignment algorithms for next-generation 5G wireless communication systems.

Acknowledgements

The authors wish to express their special thanks to Seda Ustunbas (Wireless Communication Research Laboratory, Istanbul Technical University, Turkey) for useful discussions of this chapter.

Author details

Arif Basgumus[1], Mustafa Namdar[1], Hakan Alakoca[2], Eylem Erdogan[3] and Lutfiye Durak-Ata[2]*

*Address all correspondence to: lutfiye@ieee.org

1 Department of Electrical and Electronics Engineering, Dumlupinar University, Turkey

2 Informatics Institute, Applied Informatics Department, Istanbul Technical University, Turkey

3 Department of Electrical and Electronics Engineering, Istanbul Medeniyet University, Turkey

References

[1] Panwar N, Sharma S, Singh AK. A survey on 5G: The next generation of mobile communication. Physical Communication. Mar. 2016;**18**(2):64-84

[2] Wang CX et al. Cellular architecture and key technologies for 5G wireless communication networks. IEEE Communications Magazine. Feb. 2014;**52**(2):122-130

[3] Agiwal M, Roy A, Saxena N. Next generation 5G wireless networks: A comprehensive survey. IEEE Communication Surveys and Tutorials. Feb. 2016;**18**(3):1617-1655

[4] Catak E, Durak-Ata L. Waveform design considerations for 5G wireless networks. Towards 5G Wireless Networks-A Physical Layer Perspective, InTech. Dec. 2016;**18**(3):27-48

[5] Sharma SK et al. Cognitive radio techniques under practical imperfections: A survey. IEEE Communication Surveys and Tutorials. Jul. 2015;**17**(4):1858-1884

[6] Hong X, Wang J, Wang CX, Shi J. Cognitive radio in 5G: A perspective on energy-spectral efficiency trade-off. IEEE Communications Magazine. Jul. 2014;**52**(7):46-53

[7] Zhang Z, Zhang W, Zeadally S, Wang Y, Liu Y. Cognitive radio spectrum sensing framework based on multi-agent architecture for 5G networks. IEEE Wireless Communications. Dec. 2015;**22**(6):34-39

[8] Kakalou I, Psannis KE, Krawiec P, Badea R. Cognitive radio network and network service chaining toward 5G: Challenges and requirements. IEEE Communications Magazine. Nov. 2017;**55**(11):145-151

[9] Namdar M, Basgumus A. Outage performance analysis of underlay cognitive radio networks with decode-and-forward relaying. In: Cognitive Radio. InTech; 2017. pp. 25-37

[10] Razaviyayn M, Sanjabi M, Luo Z-Q. Linear transceiver design for interference alignment: Complexity and computation. IEEE Transactions on Information Theory. May 2012;**58**(5): 2896-2910

[11] Liu T, Yang C. On the feasibility of linear interference alignment for MIMO interference broadcast channels with constant coefficients. IEEE Transactions on Signal Processing. May 2013;**61**(9):2178-2191

[12] Gonzalez O, Beltran C, Santamaria I. A feasibility test for linear interference alignment in MIMO channels with constant coefficients. IEEE Transactions on Information Theory. Mar. 2014;**60**(3):1840-1856

[13] Razaviyayn M, Gennady L, Zhi-Quan L. On the degrees of freedom achievable through interference alignment in a MIMO interference channel. IEEE Transactions on Signal Processing. Feb. 2012;**60**(2):812-821

[14] Zhao N, Yu FR, Sun H, Li M. Adaptive power allocation schemes for spectrum sharing in interference-alignment-based cognitive radio networks. IEEE Transactions on Vehicular Technology. May 2016;**65**(5):3700-3714

[15] Sam PP, Gowindaswarny UM. Antenna selection and power allocation for IA-based underlay CR. IET Signal Processing. Jun. 2017;**11**(6):734-742

[16] Sultana R, Sarkar MZI, Hossain MS. Linear precoding techniques in enhancing security of cognitive radio networks. IEEE ICECTE, Rajshahi, Bangladesh. Dec. 2016:1-4

[17] Zhao N, Yu FR, Sun H. Adaptive energy-efficient power allocation in green interference-alignment-based wireless networks. IEEE Transactions on Vehicular Technology. 2015; **64**(9):4268-4281

[18] Amir M, Keyi AE, Nafie M. Constrained interference alignment and the spatial degrees of freedom of MIMO cognitive networks. IEEE Transactions on Information Theory. May 2011;**57**(5):2994-3004

[19] Jafar SA. Interference alignment: A new look at signal dimensions in a communication network. Foundations and Trends in Communications and Information Theory. Jun. 2011; **7**(1):1-134

[20] Zhao N et al. Interference alignment and its applications: A survey, research issues, and challenges. IEEE Communication Surveys and Tutorials. Mar. 2016;**18**(3):1779-1803

[21] Chen X, Yuen C. On interference alignment with imperfect CSI: Characterizations of outage probability, ergodic rate and SER. IEEE Transactions on Vehicular Technology. Jan. 2016;**65**(1):47-58

[22] Thukral J, Bolcskei H. Interference alignment with limited feedback. IEEE ISIT, Seoul, Korea. Jul. 2009:1759-1763

[23] Song B, Hardt M. Effects of imperfect channel state information on achievable rates of precoded multi-user MIMO broadcast channels with limited feedback. IEEE ICC, Deresden, Germany. Jun. 2009:1-5

[24] Rezaee M, Guillaud M. Interference alignment with quantized grassmannian feedback in the K-user constant MIMO interference channel. IEEE Transactions on Wireless Communications. Feb. 2016;**15**(2):1456-1468

[25] Krishnamachari RT, Varanasi MK. Interference alignment under limited feedback for MIMO interference channels. IEEE Transactions on Signal Processing. Aug. 2013;**61**(15): 3908-3914

[26] Sam RP, Govindaswamy UM. Antenna selection and adaptive power allocation for IA-based underlay CR. IET Signal Processing. Jun. 2017;**11**(6):734-742

[27] Tang J, Lambotharan S, Pomeroy S. Interference cancellation and alignment techniques for multiple-input and multiple-output cognitive relay networks. IET Signal Processing. Feb. 2013;**7**(3):188-200

[28] Arzykulov S, Nauryzbayev G, Tsiftsis TA, Abdallah M. Error performance of wireless powered cognitive relay networks with interference alignment. IEEE PIMRC, Montreal, Canada. Jun. 2017:1-5

[29] Arzykulov S, Nauryzbayev G, Tsiftsis TA, Abdallah M. On the capacity of wireless powered cognitive relay network with interference alignment. IEEE PIMRC, Singapore. Dec. 2017:1-6

[30] Ata SO, Altunbas I. Analog network coding over cascaded fast fading Rayleigh channels in the presence of self-interference. IEEE SIU, Zonguldak, Turkey. May 2016:253-256

[31] Chiani M, Win MZ, Zanella A. On the capacity of spatially correlated MIMO Rayleigh-fading channels. IEEE Transactions on Information Theory. Oct. 2003;**49**(10):2363-2371

[32] Gradshteyn IS, Ryzhik IM. Table of Integrals, Series, and Products. 7th ed. Amsterdam: Elsevier/Academic Press; 2007

[33] Ghavami H, Moghaddam SS. Outage probability of device to device communications underlaying cellular network in Suzuki fading channel. IEEE Communications Letters. May 2017;**21**(5):1203-1206

[34] Toan HV, Bao VNQ, Le KN. Performance analysis of cognitive underlay two-way relay networks with interference and imperfect channel state information. EURASIP Journal on Wireless Communications and Networking. Nov. 2018;**2018**(53):1-10

[35] Zhang C, Ge J, Li J, Rui Y, Guizani M. A unified approach for calculating the outage performance of two-way AF relaying over fading channels. IEEE Transactions on Vehicular Technology. Mar. 2015;**64**(3):1218-1229

[36] Nasir A, Zhou X, Durrani S, Kennedy R. Relaying protocols for wireless energy harvesting and information processing. IEEE Transactions on Wireless Communications. Jul. 2013; **12**(7):3622-3636

[37] Sung H, Park SH, Lee KJ, Lee I. Linear precoder designs for *K*-user interference channels. IEEE Transactions on Wireless Communications. Jan. 2010;**9**(1):291-301

[38] Jindal N. MIMO broadcast channels with finite-rate feedback. IEEE Transactions on Information Theory. Nov. 2006;**52**(11):5045-5060

[39] Zhao N, Yu FR, Sun H, Li M. Adaptive power allocation schemes for spectrum sharing in interference-alignment-based cognitive radio networks. IEEE Transactions on Vehicular Technology. May 2016;**65**(5):3700-3714

[40] Afana A, Mahady IA, Ikki S. Quadrature spatial modulation in MIMO cognitive radio systems with imperfect channel estimation and limited feedback. IEEE Transactions on Communications. Mar. 2017;**65**(3):981-991

[41] Rappaport TS. Wireless Communications: Principles and Practice. 2nd ed. New Jersey: Prentice Hall; 2001

IntechOpen

IntechOpen